2.5 Multivariate methods for the signal extraction

The selection of the candidates and the signal region definition, as they are explained in the previous sections, allow a very good rejection of the reducible backgrounds and partly of the irreducible ones. Anyways, the signal region is still contaminated by events of irreducible backgrounds that must be accounted for. To further reject those events, two different MVA approaches are used and analyzed: the first one is a BDT developed for the rejection of the $t\bar{t}$ background against the HH signal, and the second is a DNN trained against all backgrounds to extract the ggHH signal. Both approaches discriminate signal from background by being trained on the processes' kinematical features. An example of the distribution of the BDT and DNN output can be seen from Fig. F.16 to F.19. The output of the BDT (DNN), referred to as *BDT (DNN) score*, is a number between -1 (0) and 1. Events getting a score closer to -1 (0) are background-like events, while those getting a score closer to 1 are signal-like events. These distributions are used for the final signal extraction which consists of a binned likelihood fit, as described in Sec. 3.1.

2.5.1 BDT for the $t\bar{t}$ background rejection

This method is based on a BDT designed for the rejection of $t\bar{t}$ events, which constitutes the largest irreducible background, against the HH signal. To develop this BDT, the TMVA toolkit [95] of the ROOT Analysis Framework [96] has been used. The gradient boost algorithm was chosen for this BDT as it proved itself the most robust against overtraining and the one giving the best discrimination. This method has been optimized for all the channels, *i.e.* $\tau_e\tau_h$, $\tau_\mu\tau_h$ and $\tau_h\tau_h$, on the 2016 data sets used in [4], exhibiting an improvement of approximately 30% in sensitivity.

A more detailed description of the BDT design, the variables used as input, and its optimization can be found in Appendix C. The complete design of this MVA method is documented in [97].

2.5.2 DNN for the signal extraction

This method is based on a DNN designed for the selection of the HH signal against the background events. The DNN is based on two discriminators, each composed of an ensemble of ten neural networks trained via ten-fold stratified cross-validation of their training data. The architecture used for the networks is: six densely connected hidden layers with swish-1 activation functions [98] and a single output neuron with sigmoid activation function. This DNN approach is still under development and possible improvements are still possible. Moreover, this approach has been validated only for the 2016 data sets and the validation over 2018 data sets is still ongoing. Nonetheless, preliminary results show that the DNN approach gives a considerable improvement w.r.t. the BDT approach.

A more detailed description of the DNN design, the variables used as input, and its optimization can be found in Appendix D.

Chapter 3

Higgs boson self-coupling limit extraction

In this chapter, we discuss the optimization of the final discriminating variable and the results obtained. We first introduce the statistical way in which the BDT and DNN scores are interpreted (Sec. 3.1 and 3.2). We then move to the detailed description of the discriminating variable distribution optimization procedure (Sec. 3.3) and all the steps that it involves. Finally, we present the optimized results (Sec. 3.4) and their comparison with earlier results (Sec. 3.5).

3.1 Statistical interpretation

Once the selections and categorization of the events have been established, a statistical procedure is needed to systematically assess the presence or absence of a signal in the observed data. The statistical framework used in this work is the frequentist approach adopted by the CMS and ATLAS Collaborations for the H analyses combination [99, 100].

The goal of a statistical test is to make a statement about how well the observed data stand in agreement with a given hypothesis. To do so, we define two hypotheses: the *null hypothesis* (H_0) describing a signal plus background model, and the *alternative hypothesis* (H_1) describing the background-only hypothesis. To make a quantitative statement about the compatibility of the data with H_0 or H_1 we need to build a function of the measured data, referred to as the *test statistic* q_μ, which ideally is distributed differently for the two hypotheses. To understand this approach, we have to introduce the concept of *likelihood function* for H_1:

$$\mathcal{L}(n|\mu s + b) = \prod_i \frac{(\mu s_i + b_i)^{n_i}}{n_i!} e^{-\mu s_i + b_i} \tag{3.1}$$

where n, s, b, μ are the observed yield, the expected signal and background yields, and the signal strength modifier, respectively. Being our study based on a binned variable, the subscript i runs on the bins of the MVA scores defined in Sec. 2.5. The signal strength modifier is defined as $\mu = (\sigma \cdot \mathcal{B})_{obs}/(\sigma \cdot \mathcal{B})_{\mathrm{SM}}$ and encodes how strong is the presence of signal in the data compared to the SM expectation. Following the convention used in SM-like H searches, we normalize the signal to $\sigma{\cdot}\mathcal{B} = 1\mathrm{pb}$. The likelihood function 3.1, gives the total probability of observing n total events, distributed as n_i events per bin i, under the hypothesis of having s total events of signal and b of background, distributed as s_i and b_i events per bin i. This formalism, however, does not include systematic uncertainties yet. Their effect is retrieved by the insertion of a set of *nuisance parameters* ν_i such that the dependence $s \equiv s(\nu)$ and $b \equiv b(\nu)$, with ν the entire set of nuisances, can be established. The nuisances estimate $\tilde{\nu_i}$, generally obtained in regions orthogonal to the HH signal regions or from a priori considerations, is used to get our degree of belief on what is the real value of ν_i as the Bayesian probability density function $\rho(\nu_i, \tilde{\nu}_i)$. We reinterpret it as a frequentist probability $p(\tilde{\nu}_i, \nu_i)$ thanks to Bayes' theorem and the usage of a flat prior. In this way, the likelihood can be generalized to contain an arbitrary number of nuisances as $\mathcal{L}(n|\mu, \nu) = \mathcal{L}(n|\mu s(\nu) + b(\nu)) \cdot p(\tilde{\nu}_i, \nu_i)$.

The Neyman-Pearson lemma states that the most powerful test we can create is a likelihood ratio. Therefore, based on this lemma we can define the following test statistics:

$$q_\mu = -2\ln\frac{\mathcal{L}(n, \tilde{\nu}|\mu, \hat{\hat{\nu}})}{\mathcal{L}(n, \tilde{\nu}|\hat{\mu}, \hat{\nu})}, \qquad \text{with} \quad 0 < \hat{\mu} < \mu \tag{3.2}$$

where $\hat{\hat{\nu}}$ is the value that maximizes $\mathcal{L}$ when μ is fixed, while $\hat{\mu}$ and $\hat{\nu}$ are the values that maximize $\mathcal{L}$ when both are left floating at the same time. The likelihood ratio appearing in 3.2 is generally referred to as *profiled likelihood ratio*.

In the absence of clear signal observation, like in the case at hand due to the smallness of the signal production cross section, the data can still be used to provide powerful information about the largest signal we can exclude. In this context, the modified frequentist approach often referred to as CL$_s$ (with CL standing for Confidence Level) is used [101, 102]. In this framework, given an observed value of the test statistics q_μ^{obs}, the CL$_s$ quantity is defined as:

$$\mathrm{CL}_s(\mu) = \frac{P(q_\mu \geq q_\mu^{obs}|H_0)}{P(q_\mu \geq q_\mu^{obs}|H_1)} \tag{3.3}$$

where at the numerator and denominator we have the probability of q_μ being larger or equal to the observed value under the H$_0$ or H$_1$ hypothesis, respectively. Having this definition, a signal strength μ is excluded at a CL α if CL$_s(\mu) < 1 - \alpha$. Following the convention, the 95% CL is always stated in the following ($\mu^{95\%}$).

All the above can also be used to extract expected limits. To this end, we create a set of pseudo-data (*i.e.* an Asimov data set [103] for which $n_i \equiv s_i + b_i$) and we apply the CL$_s$ procedure to it. To define the expected limits, we build a cumulative probability: the expected value median is the $\mu^{95\%}$ value at which the cumulative probability distribution crosses the 0.50 quantile; the $\pm 1\sigma$ and $\pm 2\sigma$ bands edges are determined at the crossing of the 0.16/0.84 and 0.025/0.975 quantiles, respectively.

3.2 Systematic uncertainties

In this analysis, we include various sources of systematic uncertainties. They can be categorized as *normalization* and *shape uncertainties*: those of the first kind affect the total yield of the event processes, while those of the latter sort affect the shape of the events' distribution by modifying the yield of the single bins separately.

3.2.1 Normalization uncertainties

- luminosity uncertainty: is experimentally measured to be 2.5% for both the 2016 and 2018 data-taking periods [104, 105], affecting all processes but QCD multijet
- objects trigger and isolation uncertainties: 3% for electrons and 6% for taus in the $\tau_e\tau_h$ channel; 2% for muons and 6% for taus in the $\tau_\mu\tau_h$ channel; 10% for taus in the $\tau_h\tau_h$ channel due to the custom tauIDSF presence [4], affecting all processes but QCD multijet
- b tag efficiency uncertainty: evaluated together with the Data/Bkg SFs is 2% for the signal; 3% for the $\mathrm{t\bar{t}}$ and Others backgrounds; 4% for the DY background; not affecting QCD multijet

- jet scale uncertainty: 2% for the signal and 4% for all the background processes but QCD multijet [4]
- tau scale uncertainty: fixed at 6%, affecting all processes but QCD multijet (estimated as the mean of the tau scale uncertainties present in [4])
- branching ratios uncertainties: theoretical uncertainties on the H branching ratios $\mathcal{B}(\mathrm{H} \to \mathrm{bb})$ amounting to +1.2/-1.3% and on $\mathcal{B}(\mathrm{H} \to \tau\tau)$ amounting to 1.6% [14]
- $\sigma^{\mathrm{ggHH}}_{\text{NNLO-FTapprox}}$ theoretical uncertainties: +2.2/-5.0% scale uncertainty, 2.6% m_t uncertainty, 2.1% PDF uncertainty and 2.1% α_S uncertainty [21]
- DY + jets SFs uncertainty: the DY background is estimated from MC simulation and tuned with data from $\mu\mu$ sidebands. The SFs uncertainty is estimated at 10%
- QCD scale uncertainty: due to not included higher-order QCD contributions to the process, amounts to +4.8/-5.5% for the $\mathrm{t\bar{t}}$ background [4]
- QCD multijet normalization: amounting to 15% and affecting only the QCD background (estimated as the mean of the QCD multijet uncertainties present in [4])

3.2.2 Shape uncertainties

- top mass uncertainty: the uncertainty on the mass of the top quark in our work affects both the ggHH production, by entering in the heavy quark loops, and the $\mathrm{t\bar{t}}$ background. In both cases, a variation of the top quark mass induces a modification of the p_{T} spectrum of the final state particles and therefore a modification of the BDT ad DNN scores too. To account for this, the BDT and DNN can be re-evaluated using the nominal mass shifted by its uncertainty
- jet energy scale (JES) and tau energy scale (TES) uncertainty: considered fully correlated with the associated normalization uncertainties, the uncertainty related to the measurement of the jets and tau energies results in a modification of the BDT ad DNN scores because both of them are trained on the kinematical variables of the particles in the final state. To account for this, the BDT and DNN can be re-evaluated using the nominal observables shifted by the energy scale variations. These two shape uncertainties were not introduced in this analysis due to the very high computational demand required for their production. In fact, during the re-evaluation of the discriminating variable, every single source of JES and TES (respectively 11 and 7) has to be considered separately both for the up and down shifting of the nominal observables. The calculation of these uncertainties is currently undergoing and they will be added in the near future

3.3 Optimization of the discriminating variable

The discriminating variables described in Sec. 2.5, *i.e.* the BDT and the DNN, are used to obtain an expected upper limit on $\sigma^{\mathrm{ggHH}} \cdot \mathcal{B}(\mathrm{HH} \to \mathrm{bb}\tau\tau)$ via a binned likelihood fit as detailed in Sec. 3.1. Since the variables are binned, part of the information is lost in the binning procedure; to make the loss of information as small as possible, I designed an optimization procedure for the binning as part of this thesis work. This optimization procedure is completely general and can be applied to any variable undergoing a binned likelihood fit.

To understand why this procedure is needed, take for example the traditional approach used for the HH $\to$ bb$\tau\tau$ analysis: a likelihood fit of the BDT distribution binned with ten bins of constant size [94]. This choice, however practical and well established, causes a huge loss of information due to the large width of the bins and, as a consequence, the expected upper limit on $\sigma^{\mathrm{ggHH}} \cdot \mathcal{B}(\mathrm{HH} \to \mathrm{bb}\tau\tau)$

Chapter 4

Conclusions

4.1 Conclusions

A study of the Higgs boson self-coupling in the HH $\rightarrow$ bb$\tau\tau$ channel has been presented. This work finds itself aligned with the particle physics community goal of the full characterization of the scalar boson, as well as with the European Strategy for Particle Physics that encourages the study of the interaction of the Higgs boson with itself.

The study has been performed using a data sample corresponding to an integrated luminosity of 95.9fb^{-1} collected with the CMS detector during the Run 2 of the LHC, for proton-proton collisions operation at a center-of-mass energy of 13 TeV. We use the bb$\tau\tau$ final state because it gives a good trade-off between a sizable branching fraction (7.3%) and the purity of the τ lepton selection.

Many improvements, compared to the old approaches, have been introduced in the current search.

The first improvement is to capitalize on the enhanced separation power of the new discriminator, *i.e.* the DNN discriminating variable for the extraction of the Higgs pair production signal against the large background. Such a discriminator is based on a deep neural network trained against the entirety of background contaminating the signal region. Moreover, we profit of the introduction of a new τ lepton reconstruction algorithm, based on the deep neural network called *DeepTau*, and of the introduction of the new b tagger based on the *DeepFlavour* neural network (both of which were developed out of the scope of this thesis).

The novel optimization procedure for the discriminating variable, used in the signal extraction, is the last improvement introduced in this analysis. This procedure was designed, developed, and validated as part of this thesis work and is the first of its kind. Such an optimization procedure is devised to extract the maximum information possible from the data collected by the CMS experiment and has proven to give considerable improvements compared to the results obtained without its application. This optimization procedure has been validated against the data sets corresponding to the 2016 and 2018 data taking periods of the LHC, for both the BDT and DNN discriminating variables. The validation shows that, for each year and each discriminating variable, the optimization procedure allows an improvement of the expected upper limits by 20% to 30%. Moreover, it produces a $\pm 2\sigma$ band narrower by 15% to 25% (compared to the ten bin benchmark).

The final optimized expected upper limit that we quote as our result is of $\sigma^{\mathrm{ggHH}} \cdot \mathcal{B}(\mathrm{HH} \rightarrow \mathrm{bb}\tau\tau) =$ 4.6$\times$SM with the respective $\pm 2\sigma$ band of [2.4, 10], obtained with an integrated luminosity of 95.9fb^{-1}. On this result, the impact of the optimization procedure is a 27% improvement of the expected upper limit, and a $\pm 2\sigma$ band 25% narrower (compared to the ten bin benchmark). This result improves the latest CMS expected upper limit by 80% and corresponds to the most stringent expected upper limit on $\sigma^{\mathrm{ggHH}} \cdot \mathcal{B}(\mathrm{HH} \rightarrow \mathrm{bb}\tau\tau)$ so far at LHC.

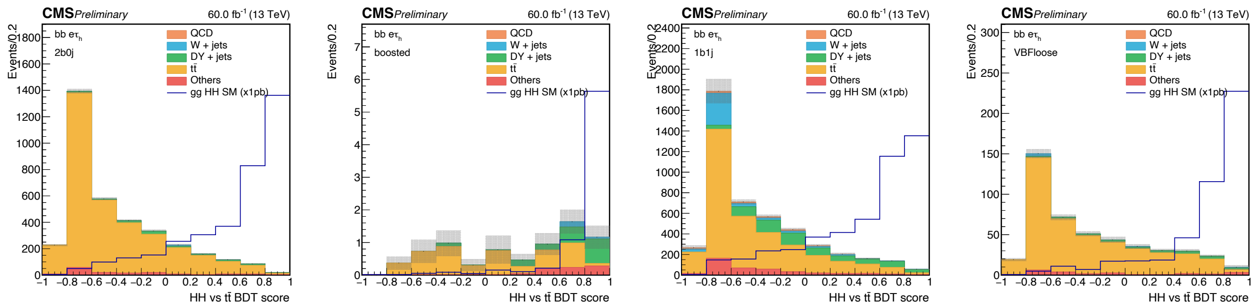

(a) $\tau_e\tau_h$

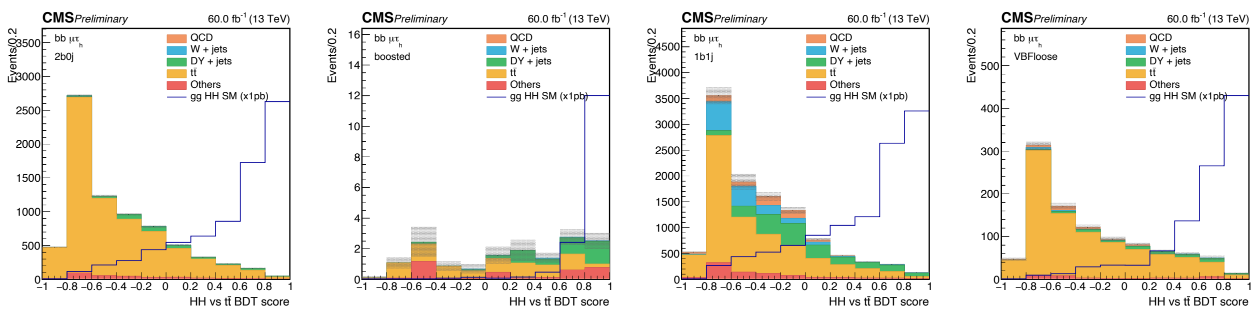

(b) $\tau_\mu\tau_h$

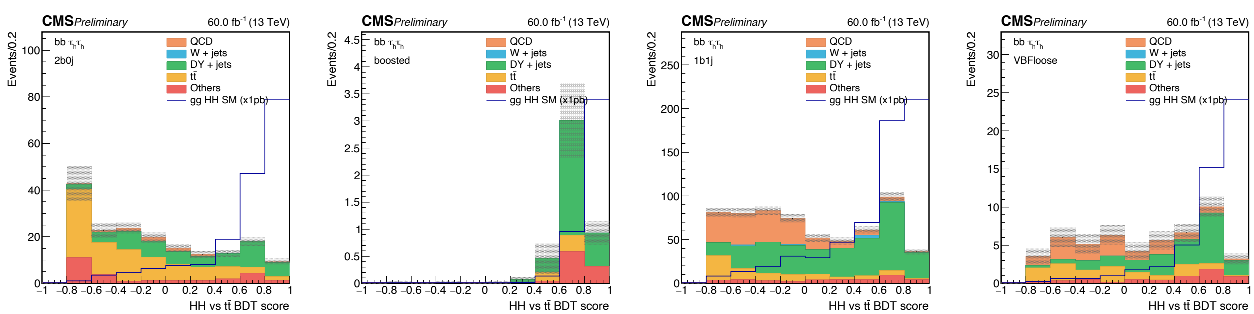

(c) $\tau_h\tau_h$

Figure F.16: *Examples of signal and background distributions of the BDT score for all the categories and channels of 2018 (the VBFtight category of the* $\tau_h\tau_h$ *channel has been omitted). A constant width binning for 10 bins has bin applied*

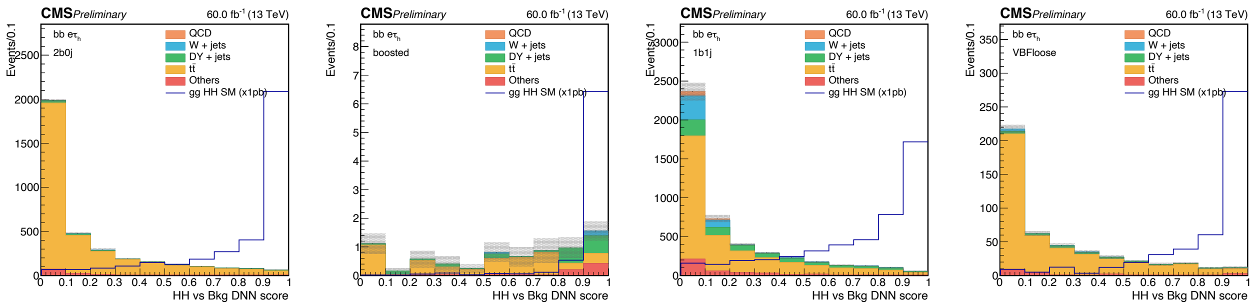

(a) $\tau_e\tau_h$

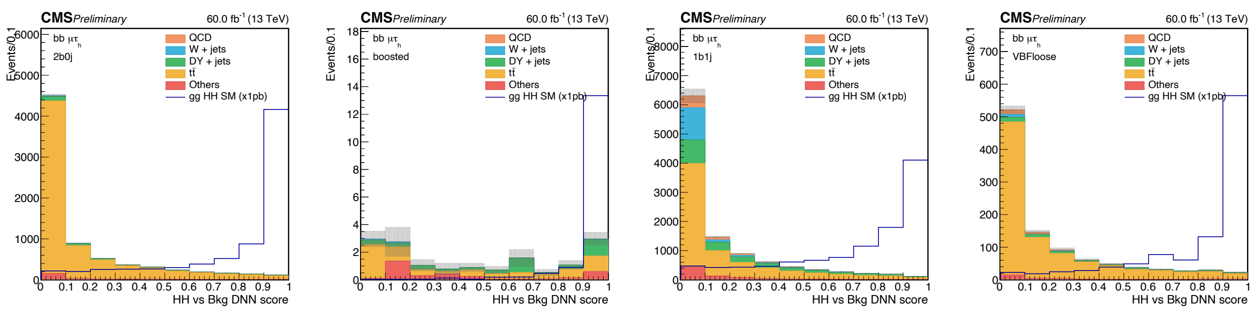

(b) $\tau_\mu\tau_h$

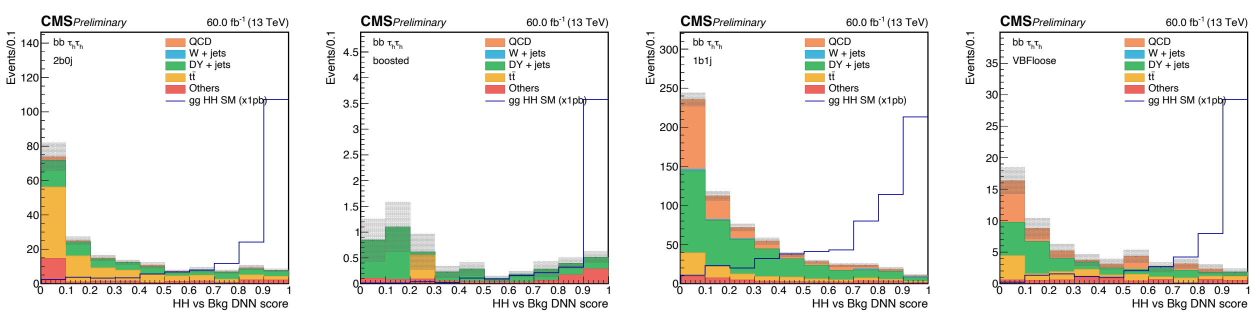

(c) $\tau_h\tau_h$

Figure F.17: *Examples of signal and background distributions of the DNN score for all the categories and channels of 2018 (the VBFtight category of the* $\tau_h\tau_h$ *channel has been omitted). A constant width binning for 10 bins has bin applied*

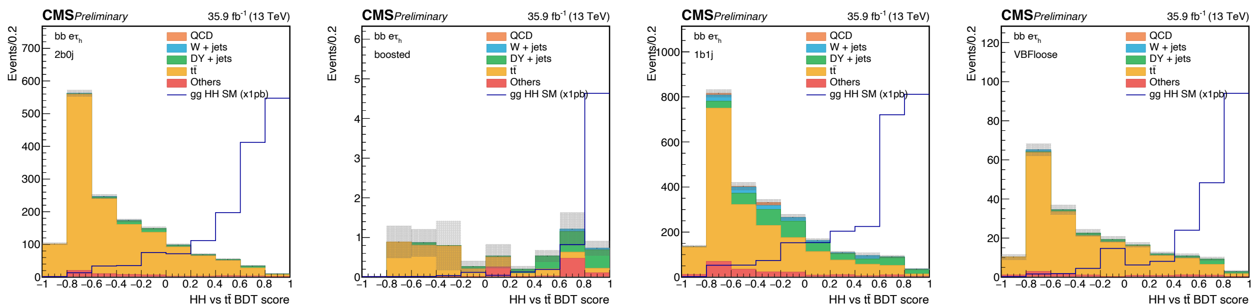

(a) $\tau_e \tau_h$

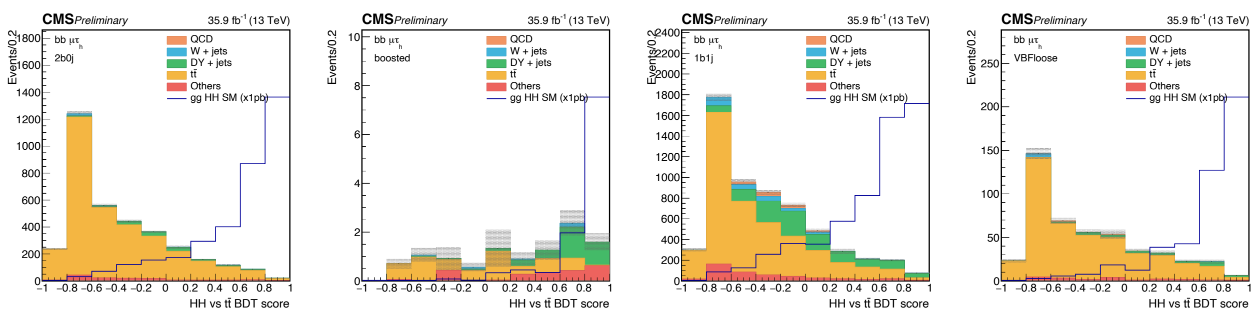

(b) $\tau_\mu \tau_h$

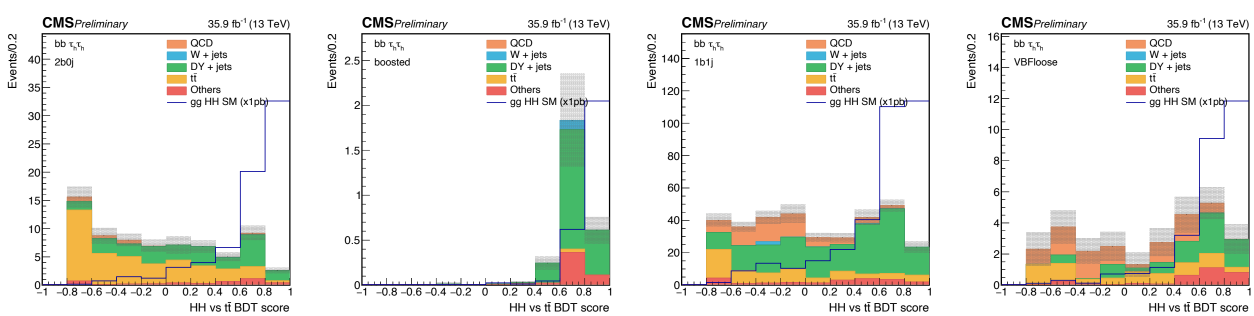

(c) $\tau_h \tau_h$

Figure F.18: *Examples of signal and background distributions of the BDT score for all the categories and channels of 2016. A constant width binning for 10 bins has bin applied*

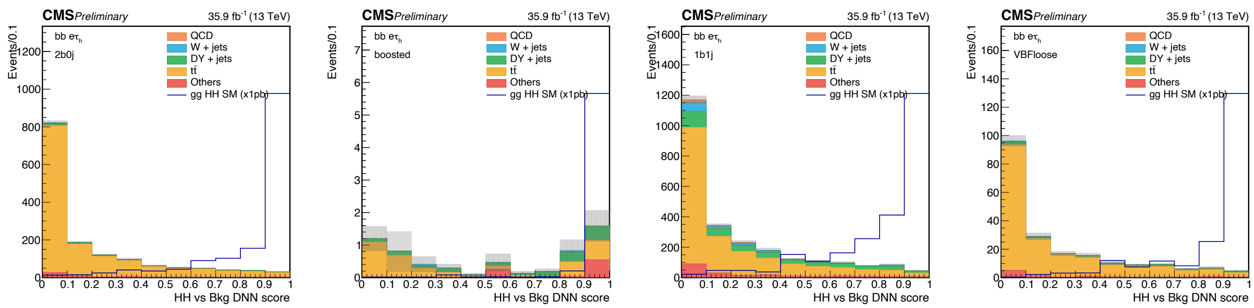

(a) $\tau_e\tau_h$

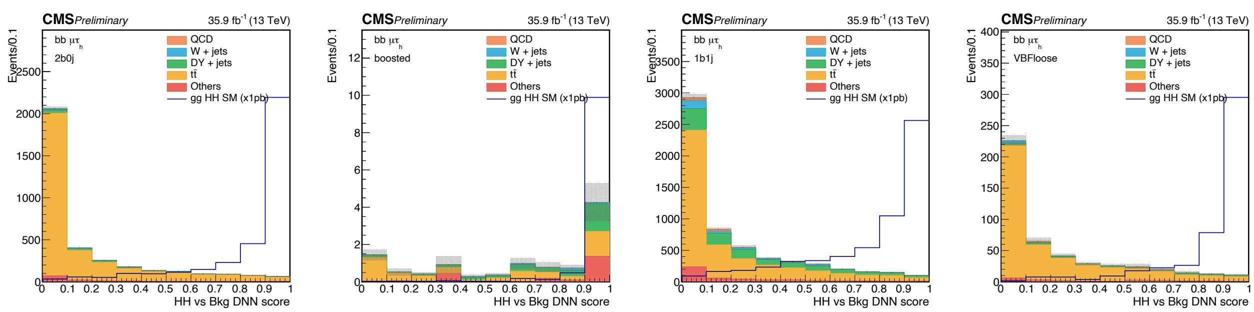

(b) $\tau_\mu\tau_h$

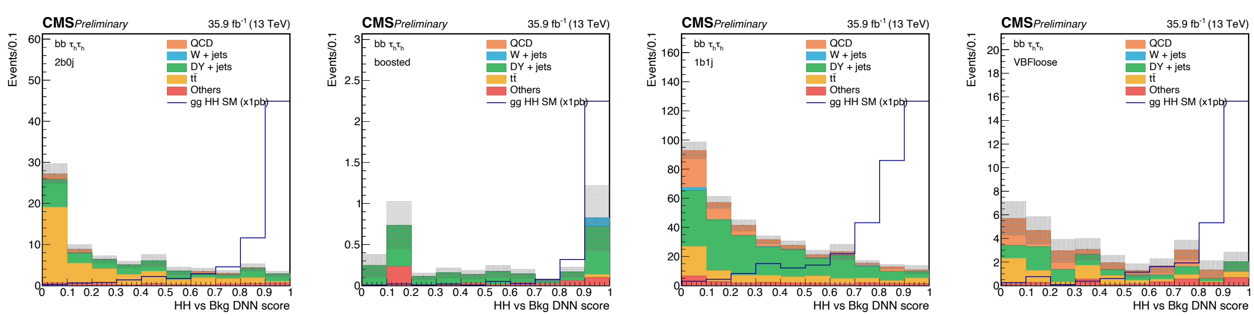

(c) $\tau_h\tau_h$

Figure F.19: *Examples of signal and background distributions of the DNN score for all the categories and channels of 2016. A constant width binning for 10/20 bins has bin applied*

Bibliography

[1] CMS Collaboration. "Observation of a new boson at a mass of 125 GeV with the CMS experiment at the LHC". In: *Phys. Lett.* B716 (2012), pp. 30–61. DOI: 10.1016/j.physletb.2012.08.021. arXiv: 1207.7235 [hep-ex].

[2] CMS Collaboration. "Observation of a new boson with mass near 125 GeV in pp collisions at $\sqrt{s} = 7$ and 8 TeV". In: *Journal of High Energy Physics* 2013.6 (June 2013). ISSN: 1029-8479. DOI: 10.1007/jhep06(2013)081. URL: http://dx.doi.org/10.1007/JHEP06(2013)081.

[3] ATLAS Collaboration. "Observation of a new particle in the search for the Standard Model Higgs boson with the ATLAS detector at the LHC". In: *Phys. Lett.* B716 (2012), pp. 1–29. DOI: 10.1016/j.physletb.2012.08.020. arXiv: 1207.7214 [hep-ex].

[4] CMS Collaboration. "Search for Higgs boson pair production in events with two bottom quarks and two tau leptons in proton–proton collisions at $\sqrt{s}$=13TeV". In: *Physics Letters B* 778 (Mar. 2018), pp. 101–127. ISSN: 0370-2693. DOI: 10.1016/j.physletb.2018.01.001. URL: http://dx.doi.org/10.1016/j.physletb.2018.01.001.

[5] S. Weinberg. "A Model of Leptons". In: *Phys. Rev. Lett.* 19 (21 Nov. 1967), pp. 1264–1266. DOI: 10.1103/PhysRevLett.19.1264. URL: https://link.aps.org/doi/10.1103/PhysRevLett.19.1264.

[6] M. Herrero. "The Standard model". In: *NATO Sci. Ser. C* 534 (1999). Ed. by T. Ferbel, pp. 1–59. DOI: 10.1007/978-94-011-4689-0_1. arXiv: hep-ph/9812242.

[7] F. Englert and R. Brout. "Broken Symmetry and the Mass of Gauge Vector Mesons". In: *Phys. Rev. Lett.* 13 (9 Aug. 1964), pp. 321–323. DOI: 10.1103/PhysRevLett.13.321. URL: https://link.aps.org/doi/10.1103/PhysRevLett.13.321.

[8] P. W. Higgs. "Broken Symmetries and the Masses of Gauge Bosons". In: *Phys. Rev. Lett.* 13 (16 Oct. 1964), pp. 508–509. DOI: 10.1103/PhysRevLett.13.508. URL: https://link.aps.org/doi/10.1103/PhysRevLett.13.508.

[9] J. Iliopoulos. "Introduction to the Standard Model of the Electro-Weak Interactions". In: *8th CERN–Latin-American School of High-Energy Physics*. 2014, pp. 1–30. DOI: 10.5170/CERN-2014-008.1. arXiv: 1305.6779 [hep-ph].

[10] F. Strocchi. "Symmetry Breaking in the Ising Model". In: *Symmetry Breaking*. Berlin, Heidelberg: Springer Berlin Heidelberg, 2008, pp. 131–138. ISBN: 978-3-540-73593-9. DOI: {10.1007/978-3-540-73593-9_21}. URL: https://doi.org/10.1007/978-3-540-73593-9_21.

[11] G. Aad et al. "Combined Measurement of the Higgs Boson Mass in pp collisions at $\sqrt{s} = 7$ and 8 TeV with the ATLAS and CMS Experiments". In: *Physical Review Letters* 114.19 (May 2015). ISSN: 1079-7114. DOI: 10.1103/physrevlett.114.191803. URL: http://dx.doi.org/10.1103/PhysRevLett.114.191803.

[12] V. Khachatryan et al. "Precise determination of the mass of the Higgs boson and tests of compatibility of its couplings with the standard model predictions using proton collisions at 7 and 8 TeV". In: *The European Physical Journal C* 75.5 (May 2015). ISSN: 1434-6052. DOI: 10.1140/epjc/s10052-015-3351-7. URL: http://dx.doi.org/10.1140/epjc/s10052-015-3351-7.

[13] E. Glover and J. van der Bij. "Higgs boson pair production via gluon fusion". In: *Nuclear Physics B* 309.2 (1988), pp. 282–294. ISSN: 0550-3213. DOI: https://doi.org/10.1016/0550-3213(88)90083-1. URL: http://www.sciencedirect.com/science/article/pii/0550321388900831.

[14] D. de Florian et al. "Handbook of LHC Higgs Cross Sections: 4. Deciphering the Nature of the Higgs Sector". In: *CERN Yellow Reports: Monographs - Volume 2/2017* (2016). arXiv: 1610.07922 [hep-ph].

[15] A. Djouadi et al. "Production of neutral Higgs-boson pairs at LHC". In: *The European Physical Journal C* 10.1 (Aug. 1999), pp. 45–49. ISSN: 1434-6052. DOI: 10.1007/s100529900083. URL: http://dx.doi.org/10.1007/s100529900083.

[16] J. Baglio et al. "The measurement of the Higgs self-coupling at the LHC: theoretical status". In: *Journal of High Energy Physics* 2013.4 (Apr. 2013). ISSN: 1029-8479. DOI: 10.1007/jhep04(2013)151. URL: http://dx.doi.org/10.1007/JHEP04(2013)151.

[17] R. Frederix et al. "Higgs pair production at the LHC with NLO and parton-shower effects". In: *Physics Letters B* 732 (May 2014), pp. 142–149. ISSN: 0370-2693. DOI: 10.1016/j.physletb.2014.03.026. URL: http://dx.doi.org/10.1016/j.physletb.2014.03.026.

[18] D. de Florian and J. Mazzitelli. "Higgs pair production at next-to-next-to-leading logarithmic accuracy at the LHC". In: *JHEP* 09 (2015), p. 053. DOI: 10.1007/JHEP09(2015)053. arXiv: 1505.07122 [hep-ph].

[19] S. Borowka et al. "Full top quark mass dependence in Higgs boson pair production at NLO". In: *Journal of High Energy Physics* 2016.10 (Oct. 2016). ISSN: 1029-8479. DOI: 10.1007/jhep10(2016)107. URL: http://dx.doi.org/10.1007/JHEP10(2016)107.

[20] D. de Florian et al. "Differential Higgs boson pair production at next-to-next-to-leading order in QCD". In: *Journal of High Energy Physics* 2016.9 (Sept. 2016). ISSN: 1029-8479. DOI: 10.1007/jhep09(2016)151. URL: http://dx.doi.org/10.1007/JHEP09(2016)151.

[21] M. Grazzini et al. "Higgs boson pair production at NNLO with top quark mass effects". In: *Journal of High Energy Physics* 2018.5 (May 2018). ISSN: 1029-8479. DOI: 10.1007/jhep05(2018)059. URL: http://dx.doi.org/10.1007/JHEP05(2018)059.

[22] F. Maltoni et al. "Top-quark mass effects in double and triple Higgs production in gluon-gluon fusion at NLO". In: *Journal of High Energy Physics* 2014.11 (Nov. 2014). ISSN: 1029-8479. DOI: 10.1007/jhep11(2014)079. URL: http://dx.doi.org/10.1007/JHEP11(2014)079.

[23] L. Ling et al. "NNLO QCD corrections to Higgs pair production via vector boson fusion at hadron colliders". In: *Physical Review D* 89.7 (Mar. 2014). ISSN: 1550-2368. DOI: 10.1103/physrevd.89.073001. URL: http://dx.doi.org/10.1103/PhysRevD.89.073001.

[24] M. J. Dolan et al. "Further on up the road: hhjj production at the LHC". In: *Physical Review Letters* 112.10 (Mar. 2014). ISSN: 1079-7114. DOI: 10.1103/physrevlett.112.101802. URL: http://dx.doi.org/10.1103/PhysRevLett.112.101802.

[25] M. J. Dolan et al. "hhjj production at the LHC". In: *The European Physical Journal C* 75.8 (Aug. 2015). ISSN: 1434-6052. DOI: 10.1140/epjc/s10052-015-3622-3. URL: http://dx.doi.org/10.1140/epjc/s10052-015-3622-3.

[26] J. Nakamura and J. Baglio. “Jet azimuthal angle correlations in the production of a Higgs boson pair plus two jets at hadron colliders”. In: *The European Physical Journal C* 77.1 (Jan. 2017). ISSN: 1434-6052. DOI: 10.1140/epjc/s10052-017-4593-3. URL: http://dx.doi.org/10.1140/epjc/s10052-017-4593-3.

[27] F. A. Dreyer and A. Karlberg. “Vector-boson fusion Higgs pair production at N3LO”. In: *Physical Review D* 98.11 (Dec. 2018). ISSN: 2470-0029. DOI: 10.1103/physrevd.98.114016. URL: http://dx.doi.org/10.1103/PhysRevD.98.114016.

[28] M. J. Dolan et al. “New physics in LHC Higgs boson pair production”. In: *Physical Review D* 87.5 (Mar. 2013). ISSN: 1550-2368. DOI: 10.1103/physrevd.87.055002. URL: http://dx.doi.org/10.1103/PhysRevD.87.055002.

[29] G. Heinrich et al. “Probing the trilinear Higgs boson coupling in di-Higgs production at NLO QCD including parton shower effects”. In: *Journal of High Energy Physics* 2019.6 (June 2019). ISSN: 1029-8479. DOI: 10.1007/jhep06(2019)066. URL: http://dx.doi.org/10.1007/JHEP06(2019)066.

[30] C. Chen et al. “Top partners and Higgs boson production”. In: *Physical Review D* 90.3 (Aug. 2014). ISSN: 1550-2368. DOI: 10.1103/physrevd.90.035016. URL: http://dx.doi.org/10.1103/PhysRevD.90.035016.

[31] A. Falkowski. “Effective field theory approach to LHC Higgs data”. In: *Pramana* 87.3 (Aug. 2016). ISSN: 0973-7111. DOI: 10.1007/s12043-016-1251-5. URL: http://dx.doi.org/10.1007/s12043-016-1251-5.

[32] A. Azatov et al. “Effective field theory analysis of double Higgs production via gluon fusion”. In: *CERN-PH-TH-2015-015* (2015). arXiv: 1502.00539 [hep-ph].

[33] F. Goertz et al. “Higgs boson pair production in the D = 6 extension of the SM”. In: *Journal of High Energy Physics* 2015.4 (May 2015). ISSN: 1029-8479. DOI: 10.1007/jhep04(2015)167. URL: http://dx.doi.org/10.1007/JHEP04(2015)167.

[34] R. Gröber et al. “NLO QCD corrections to Higgs pair production including dimension-6 operators”. In: *Journal of High Energy Physics* 2015.9 (Sept. 2015). ISSN: 1029-8479. DOI: 10.1007/jhep09(2015)092. URL: http://dx.doi.org/10.1007/JHEP09(2015)092.

[35] A. Carvalho et al. “Analytical parametrization and shape classification of anomalous HH production in the EFT approach”. In: *LHCHXSWG-2016-001* (2016). arXiv: 1608.06578 [hep-ph].

[36] K. Agashe et al. “The minimal composite Higgs model”. In: *Nuclear Physics B* 719.1-2 (July 2005), pp. 165–187. ISSN: 0550-3213. DOI: 10.1016/j.nuclphysb.2005.04.035. URL: http://dx.doi.org/10.1016/j.nuclphysb.2005.04.035.

[37] G. F. Giudice et al. “The strongly-interacting light Higgs”. In: *Journal of High Energy Physics* 2007.06 (June 2007), pp. 045–045. ISSN: 1029-8479. DOI: 10.1088/1126-6708/2007/06/045. URL: http://dx.doi.org/10.1088/1126-6708/2007/06/045.

[38] T. Abe et al. “Minimal dilaton model”. In: *Physical Review D* 86.11 (Dec. 2012). ISSN: 1550-2368. DOI: 10.1103/physrevd.86.115016. URL: http://dx.doi.org/10.1103/PhysRevD.86.115016.

[39] B. Bellazzini et al. “A higgs-like dilaton”. In: *The European Physical Journal C* 73.2 (Feb. 2013). ISSN: 1434-6052. DOI: 10.1140/epjc/s10052-013-2333-x. URL: http://dx.doi.org/10.1140/epjc/s10052-013-2333-x.

[40] S. Matsuzaki and K. Yamawaki. “Holographic technidilaton at 125GeV”. In: *Physical Review D* 86.11 (Dec. 2012). ISSN: 1550-2368. DOI: 10.1103/physrevd.86.115004. URL: http://dx.doi.org/10.1103/PhysRevD.86.115004.

[41] S. Matsuzaki and K. Yamawaki. “Is 125 GeV techni-dilaton found at LHC?” In: *Physics Letters B* 719.4-5 (Feb. 2013), pp. 378–382. ISSN: 0370-2693. DOI: 10.1016/j.physletb.2013.01.031. URL: http://dx.doi.org/10.1016/j.physletb.2013.01.031.

[42] J. Ellis et al. “Generalized skyrmions in QCD and the electroweak sector”. In: *Journal of High Energy Physics* 2013.3 (Mar. 2013). ISSN: 1029-8479. DOI: 10.1007/jhep03(2013)163. URL: http://dx.doi.org/10.1007/JHEP03(2013)163.

[43] Z. Chacko et al. “Resonance at 125GeV: Higgs or dilaton/radion?” In: *Journal of High Energy Physics* 2013.4 (Apr. 2013). ISSN: 1029-8479. DOI: 10.1007/jhep04(2013)015. URL: http://dx.doi.org/10.1007/JHEP04(2013)015.

[44] B. Patt and F. Wilczek. “Higgs-field portal into hidden sectors”. In: *MIT-CTP-3745* (May 2006). arXiv: hep-ph/0605188.

[45] C. Englert et al. “LHC: Standard Higgs and hidden Higgs”. In: *Physics Letters B* 707.5 (2012), pp. 512–516. ISSN: 0370-2693. DOI: https://doi.org/10.1016/j.physletb.2011.12.067. URL: http://www.sciencedirect.com/science/article/pii/S0370269312000020.

[46] B. Hespel et al. “Higgs pair production via gluon fusion in the Two-Higgs-Doublet Model”. In: *Journal of High Energy Physics* 2014.9 (Sept. 2014). ISSN: 1029-8479. DOI: 10.1007/jhep09(2014)124. URL: http://dx.doi.org/10.1007/JHEP09(2014)124.

[47] H. E. Haber and O. Stål. “New LHC benchmarks for the $\mathcal{CP}$-conserving two-Higgs-doublet model”. In: *The European Physical Journal C* 75.10 (Oct. 2015). ISSN: 1434-6052. DOI: 10.1140/epjc/s10052-015-3697-x. URL: http://dx.doi.org/10.1140/epjc/s10052-015-3697-x.

[48] J. Alison et al. “Higgs Boson Pair Production at Colliders: Status and Perspectives”. In: *Double Higgs Production at Colliders*. Ed. by B. Di Micco et al. Sept. 2019. arXiv: 1910.00012 [hep-ph].

[49] CMS Collaboration. “Search for a heavy pseudoscalar Higgs boson decaying into a 125 GeV Higgs boson and a Z boson in final states with two tau and two light leptons at $\sqrt{s} = 13$ TeV”. In: *Journal of High Energy Physics* 2020.3 (Mar. 2020). ISSN: 1029-8479. DOI: 10.1007/jhep03(2020)065. URL: http://dx.doi.org/10.1007/JHEP03(2020)065.

[50] CMS Collaboration. “Search for new neutral Higgs bosons through the $\mathrm{H} \to \mathrm{ZA} \to \ell^+\ell^-\mathrm{b\bar{b}}$ process in pp collisions at $\sqrt{s} = 13$ TeV”. In: *Journal of High Energy Physics* 2020.3 (Mar. 2020). ISSN: 1029-8479. DOI: 10.1007/jhep03(2020)055. URL: http://dx.doi.org/10.1007/JHEP03(2020)055.

[51] CMS Collaboration. “Search for heavy Higgs bosons decaying to a top quark pair in proton-proton collisions at $\sqrt{s} = 13$ TeV”. In: *Journal of High Energy Physics* 2020.4 (Apr. 2020). ISSN: 1029-8479. DOI: 10.1007/jhep04(2020)171. URL: http://dx.doi.org/10.1007/JHEP04(2020)171.

[52] CMS Collaboration. “Search for MSSM Higgs bosons decaying to $\mu^+\mu^-$ in proton-proton collisions at $\sqrt{s}$=13TeV”. In: *Physics Letters B* 798 (2019), p. 134992. ISSN: 0370-2693. DOI: https://doi.org/10.1016/j.physletb.2019.134992. URL: http://www.sciencedirect.com/science/article/pii/S0370269319307142.

[53] CMS Collaboration. “Search for heavy Higgs bosons decaying to a top quark pair in proton-proton collisions at $\sqrt{s} = 13$ TeV”. In: *Journal of High Energy Physics* 2020.4 (Apr. 2020). ISSN: 1029-8479. DOI: 10.1007/jhep04(2020)171. URL: http://dx.doi.org/10.1007/JHEP04(2020)171.

[54] CMS Collaboration. "Search for a heavy pseudoscalar boson decaying to a Z and a Higgs boson at $\sqrt{s} = 13\,\text{TeV}$". In: *The European Physical Journal C* 79.7 (July 2019). ISSN: 1434-6052. DOI: 10.1140/epjc/s10052-019-7058-z. URL: http://dx.doi.org/10.1140/epjc/s10052-019-7058-z.

[55] CMS Collaboration. "Search for additional neutral MSSM Higgs bosons in the $\tau\tau$ final state in proton-proton collisions at $\sqrt{s} = 13\text{TeV}$". In: *Journal of High Energy Physics* 2018.9 (Sept. 2018). ISSN: 1029-8479. DOI: 10.1007/jhep09(2018)007. URL: http://dx.doi.org/10.1007/JHEP09(2018)007.

[56] CMS Collaboration. "Search for beyond the standard model Higgs bosons decaying into a $b\overline{b}$ pair in pp collisions at $\sqrt{s} = 13$ TeV". In: *Journal of High Energy Physics* 2018.8 (Aug. 2018). ISSN: 1029-8479. DOI: 10.1007/jhep08(2018)113. URL: http://dx.doi.org/10.1007/JHEP08(2018)113.

[57] CMS Collaboration. "Search for a new scalar resonance decaying to a pair of Z bosons in proton-proton collisions at $\sqrt{s} = 13$ TeV". In: *Journal of High Energy Physics* 2018.6 (June 2018). ISSN: 1029-8479. DOI: 10.1007/jhep06(2018)127. URL: http://dx.doi.org/10.1007/JHEP06(2018)127.

[58] ATLAS Collaboration. "Search for charged Higgs bosons decaying into top and bottom quarks at $\sqrt{s} = 13\text{TeV}$ with the ATLAS detector". In: *Journal of High Energy Physics* 2018.11 (Nov. 2018). ISSN: 1029-8479. DOI: 10.1007/jhep11(2018)085. URL: http://dx.doi.org/10.1007/JHEP11(2018)085.

[59] ATLAS Collaboration. "Search for charged Higgs bosons decaying via $H^{\pm} \to \tau^{\pm}\nu_{\tau}$ in the τ+jets and τ+lepton final states with 36 fb^{-1} of pp collision data recorded at $\sqrt{s} = 13\text{TeV}$ with the ATLAS experiment". In: *Journal of High Energy Physics* 2018.9 (Sept. 2018). ISSN: 1029-8479. DOI: 10.1007/jhep09(2018)139. URL: http://dx.doi.org/10.1007/JHEP09(2018)139.

[60] ATLAS Collaboration. "Search for doubly charged Higgs boson production in multi-lepton final states with the ATLAS detector using proton–proton collisions at $\sqrt{s} = 13\,\text{TeV}$". In: *The European Physical Journal C* 78.3 (Mar. 2018). ISSN: 1434-6052. DOI: 10.1140/epjc/s10052-018-5661-z. URL: http://dx.doi.org/10.1140/EPJC/S10052-018-5661-Z.

[61] ATLAS Collaboration. "Search for doubly charged scalar bosons decaying into same-sign W boson pairs with the ATLAS detector". In: *The European Physical Journal C* 79.1 (Jan. 2019). ISSN: 1434-6052. DOI: 10.1140/epjc/s10052-018-6500-y. URL: http://dx.doi.org/10.1140/epjc/s10052-018-6500-y.

[62] CMS Collaboration. "Search for a light charged Higgs boson in the $H^{\pm} \to cs$ channel in proton-proton collisions at $\sqrt{s} = 13$ TeV". In: *CERN-EP-2020-057* (2020). arXiv: 2005.08900 [hep-ex].

[63] CMS Collaboration. "Search for charged Higgs bosons decaying into a top and a bottom quark in the all-jet final state of pp collisions at $\sqrt{s} = 13$ TeV". In: *CERN-EP-2020-057* (2020). arXiv: 2001.07763 [hep-ex].

[64] CMS Collaboration. "Search for a charged Higgs boson decaying into top and bottom quarks in events with electrons or muons in proton-proton collisions at $\sqrt{\text{s}} = 13$ TeV". In: *Journal of High Energy Physics* 2020.1 (Jan. 2020). ISSN: 1029-8479. DOI: 10.1007/jhep01(2020)096. URL: http://dx.doi.org/10.1007/JHEP01(2020)096.

[65] CMS Colaboration. "Search for charged Higgs bosons in the $H^{\pm} \to \tau^{\pm}\nu_{\tau}$ decay channel in proton-proton collisions at $\sqrt{s} = 13$ TeV". In: *Journal of High Energy Physics* 2019.7 (July 2019). ISSN: 1029-8479. DOI: 10.1007/jhep07(2019)142. URL: http://dx.doi.org/10.1007/JHEP07(2019)142.

[66] CMS Collaboration. "Search for a charged Higgs boson decaying to charm and bottom quarks in proton-proton collisions at $\sqrt{s} = 8$ TeV". In: *Journal of High Energy Physics* 2018.11 (Nov. 2018). ISSN: 1029-8479. DOI: 10.1007/jhep11(2018)115. URL: http://dx.doi.org/10.1007/JHEP11(2018)115.

[67] CMS Colaboration. "Combination of Searches for Higgs Boson Pair Production in Proton-Proton Collisions at $\sqrt{s}$=13TeV". In: *Physical Review Letters* 122.12 (Mar. 2019). ISSN: 1079-7114. DOI: 10.1103/physrevlett.122.121803. URL: http://dx.doi.org/10.1103/PhysRevLett.122.121803.

[68] CMS Collaboration. "The CMS Experiment at the CERN LHC". In: *JINST* 3 (2008), S08004. DOI: 10.1088/1748-0221/3/08/S08004.

[69] ATLAS Collaboration. "The ATLAS Experiment at the CERN Large Hadron Collider". In: *Journal of Instrumentation* 3.08 (Aug. 2008), S08003–S08003. DOI: 10.1088/1748-0221/3/08/s08003. URL: https://doi.org/10.1088%2F1748-0221%2F3%2F08%2Fs08003.

[70] LHCb Collaboration. "The LHCb Detector at the LHC". In: *Journal of Instrumentation* 3.08 (Aug. 2008), S08005–S08005. DOI: 10.1088/1748-0221/3/08/s08005. URL: https://doi.org/10.1088%2F1748-0221%2F3%2F08%2Fs08005.

[71] ALICE Collaboration. "The ALICE experiment at the CERN LHC". In: *Journal of Instrumentation* 3.08 (Aug. 2008), S08002–S08002. DOI: 10.1088/1748-0221/3/08/s08002. URL: https://doi.org/10.1088%2F1748-0221%2F3%2F08%2Fs08002.

[72] CMS Collaboration. "Particle-flow reconstruction and global event description with the CMS detector". In: *Journal of Instrumentation* 12.10 (Aug. 2017), P10003–P10003. DOI: 10.1088/1748-0221/12/10/p10003. URL: https://doi.org/10.1088%2F1748-0221%2F12%2F10%2Fp10003.

[73] CMS Collaboration. "Performance of the CMS muon detector and muon reconstruction with proton-proton collisions at $\sqrt{s} = 13$ TeV". In: *JINST* 13.06 (2018), P06015. DOI: 10.1088/1748-0221/13/06/P06015.

[74] CMS Collaboration. "Electron and photon performance in CMS with the full 2016 data sample." In: *CMS-DP-2017-004* (Mar. 2017). URL: https://cds.cern.ch/record/2255497.

[75] CMS Collaboration. "Performance of Electron and Photon reconstruction in the 2017 Legacy dataset of the CMS Experiment". In: *CMS-DP-2020-024* (May 2020). URL: https://cds.cern.ch/record/2718815.

[76] CMS Collaboration. "Electron and Photon performance in CMS with the data sample collected in 2016-17-18 at 13 TeV for the ICHEP 2018 Conference". In: *CMS-DP-2018-041* (July 2018). URL: https://cds.cern.ch/record/2629363.

[77] M. Tanabashi and others (Particle Data Group). "Review of Particle Physics". In: *Phys. Rev. D* 98 (3 Aug. 2018), p. 030001. DOI: 10.1103/PhysRevD.98.030001. URL: https://link.aps.org/doi/10.1103/PhysRevD.98.030001.

[78] CMS Collaboration. "Performance of τ-lepton reconstruction and identification in CMS". In: *Journal of Instrumentation* 7.01 (Jan. 2012), P01001–P01001. ISSN: 1748-0221. DOI: 10.1088/1748-0221/7/01/p01001. URL: http://dx.doi.org/10.1088/1748-0221/7/01/P01001.

[79] CMS Collaboration. "Reconstruction and identification of τ lepton decays to hadrons and ν_τ at CMS". In: *Journal of Instrumentation* 11.01 (Jan. 2016), P01019–P01019. ISSN: 1748-0221. DOI: 10.1088/1748-0221/11/01/p01019. URL: http://dx.doi.org/10.1088/1748-0221/11/01/P01019.

[80] CMS Collaboration. "Tau trigger performances at 13 TeV with 2015 data". In: *CMS-DP-2016-037* (May 2016). URL: https://cds.cern.ch/record/2195775.

[81] CMS Collaboration. "Performance of tau identification with 2016 data at $\sqrt{s} = 13$ TeV". In: *CMS-DP-2017-006* (Mar. 2017). URL: https://cds.cern.ch/record/2255737.

[82] CMS Collaboration. "Performance of reconstruction and identification of τ leptons in their decays to hadrons and ν_τ in LHC Run-2". In: *CMS PAS TAU-16-002* (July 2016). URL: https://cds.cern.ch/record/2196972.

[83] M. Cacciari et al. "The anti-ktjet clustering algorithm". In: *Journal of High Energy Physics* 2008.04 (Apr. 2008), pp. 063–063. ISSN: 1029-8479. DOI: 10.1088/1126-6708/2008/04/063. URL: http://dx.doi.org/10.1088/1126-6708/2008/04/063.

[84] M. Cacciari et al. "FastJet user manual". In: *The European Physical Journal C* 72.3 (Mar. 2012). ISSN: 1434-6052. DOI: 10.1140/epjc/s10052-012-1896-2. URL: http://dx.doi.org/10.1140/epjc/s10052-012-1896-2.

[85] CMS Collaboration. "Jet energy scale and resolution in the CMS experiment in pp collisions at 8 TeV". In: *Journal of Instrumentation* 12.02 (Feb. 2017), P02014–P02014. ISSN: 1748-0221. DOI: 10.1088/1748-0221/12/02/p02014. URL: http://dx.doi.org/10.1088/1748-0221/12/02/P02014.

[86] CMS Collaboration. "Determination of jet energy calibration and transverse momentum resolution in CMS". In: *Journal of Instrumentation* 6.11 (Nov. 2011), P11002–P11002. ISSN: 1748-0221. DOI: 10.1088/1748-0221/6/11/p11002. URL: http://dx.doi.org/10.1088/1748-0221/6/11/P11002.

[87] CMS Collaboration. "Jet algorithms performance in 13 TeV data". In: *CMS-PAS-JME-16-003* (Mar. 2017). URL: http://cds.cern.ch/record/2256875.

[88] CMS Collaboration. "Jet energy scale and resolution performance with 13 TeV data collected by CMS in 2016-2018". In: *CMS-DP-2020-019* (Apr. 2020). URL: https://cds.cern.ch/record/2715872.

[89] CMS Collaboration. "Performance of b tagging algorithms in proton-proton collisions at 13 TeV with Phase 1 CMS detector". In: *CMS-DP-2018-033* (June 2018). URL: https://cds.cern.ch/record/2627468.

[90] CMS Collaboration. "Performance of the DeepJet b tagging algorithm using 41.9/fb of data from proton-proton collisions at 13TeV with Phase 1 CMS detector". In: *CMS-DP-2018-058* (Nov. 2018). URL: https://cds.cern.ch/record/2646773.

[91] CMS Collaboration. "Performance of the DeepTau algorithm for the discrimination of taus against jets, electron, and muons". In: *CMS-DP-2019-033* (Oct. 2019). URL: http://cds.cern.ch/record/2694158.

[92] K. Androsov for the CMS Collaboration. "Identification of tau leptond using deep learning techniques at CMS". In: *Proceedings of the 27th International Symposium Nuclear Electronics and Computing (NEC'2019) Budva, Becici, Montenegro, September 30 – October 4, 2019* (Oct. 2019). URL: http://ceur-ws.org/Vol-2507/84-88-paper-13.pdf.

[93] L. Bianchini et al. "Reconstruction of the Higgs mass in $H \to \tau\tau$ Events by Dynamical Likelihood techniques". In: *J. Phys. Conf. Ser.* 513 (2014), p. 022035. DOI: 10.1088/1742-6596/513/2/022035.

[94] C. Amendola. "Vector Boson Fusion trigger and search for Higgs boson pair production at the LHC in the bb$\tau\tau$ channel with the CMS detector". PhD thesis. Dec. 2019.

[95] A. Hoecker et al. "TMVA - Toolkit for Multivariate Data Analysis". In: *PoS* ***ACAT*** (2007). arXiv: physics/0703039 [physics.data-an].

[96] R. Brun and F. Rademakers. "ROOT — An object oriented data analysis framework". In: *Nuclear Instruments and Methods in Physics Research Section A: Accelerators, Spectrometers, Detectors and Associated Equipment* 389.1 (1997). New Computing Techniques in Physics Research V, pp. 81–86. ISSN: 0168-9002. DOI: https://doi.org/10.1016/S0168-9002(97)00048-X. URL: http://www.sciencedirect.com/science/article/pii/S016890029700048X.

[97] A. Giraldi. "Optimisation of a multivariate analysis technique for the $t\bar{t}$ background rejection in the search for Higgs boson pair production in $b\bar{b}\tau^+\tau^-$ decay channel with the CMS experiment at the LHC". PhD thesis. Mar. 2018.

[98] P. Ramachandran et al. "Searching for Activation Functions". URL: https://arxiv.org/abs/1710.05941.

[99] ATLAS Collaboration, CMS Collaboration, and LHC Higgs Combination Group. "Procedure for the LHC Higgs boson search combination in Summer 2011". In: *CMS-NOTE-2011-005* CMS-NOTE-2011-005. ATL-PHYS-PUB-2011-11 (Aug. 2011). URL: https://cds.cern.ch/record/1379837.

[100] G. Cowan et al. "Asymptotic formulae for likelihood-based tests of new physics". In: *The European Physical Journal C* 71.2 (Feb. 2011). ISSN: 1434-6052. DOI: 10.1140/epjc/s10052-011-1554-0. URL: http://dx.doi.org/10.1140/epjc/s10052-011-1554-0.

[101] T. Junk. "Confidence level computation for combining searches with small statistics". In: *Nuclear Instruments and Methods in Physics Research Section A: Accelerators, Spectrometers, Detectors and Associated Equipment* 434.2-3 (Sept. 1999), pp. 435–443. ISSN: 0168-9002. DOI: 10.1016/s0168-9002(99)00498-2. URL: http://dx.doi.org/10.1016/S0168-9002(99)00498-2.

[102] A. L. Read. "Presentation of search results: the CLs technique". In: *Journal of Physics G: Nuclear and Particle Physics* 28.10 (Sept. 2002), pp. 2693–2704. DOI: 10.1088/0954-3899/28/10/313. URL: https://doi.org/10.1088%2F0954-3899%2F28%2F10%2F313.

[103] G. Cowan et al. "Asymptotic formulae for likelihood-based tests of new physics". In: *Eur. Phys. J.* C71 (2011). [Erratum: Eur. Phys. J.C73,2501(2013)], p. 1554. DOI: 10.1140/epjc/s10052-011-1554-0,10.1140/epjc/s10052-013-2501-z. eprint: 1007.1727.

[104] CMS Collaboration. "CMS Luminosity Measurements for the 2016 Data Taking Period". In: *CMS-PAS-LUM-17-001* (2017). URL: https://cds.cern.ch/record/2257069.

[105] CMS Collaboration. "CMS luminosity measurement for the 2018 data-taking period at $\sqrt{s} =$ 13 TeV". In: *CMS-PAS-LUM-18-002* (2019). URL: https://cds.cern.ch/record/2676164.

[106] R. Barlow and C. Beeston. "Fitting using finite Monte Carlo samples". In: *Computer Physics Communications* 77.2 (1993), pp. 219–228. ISSN: 0010-4655. DOI: https://doi.org/10.1016/0010-4655(93)90005-W.

[107] CMS Collaboration. "Measurement of Higgs boson production and decay to the $\tau\tau$ final state". In: *CMS-PAS-HIG-18-032* (2019). URL: https://cds.cern.ch/record/2668685.

[108] A Barr et al. "Di-Higgs final states augMT2ed – Selecting hh events at the high luminosity LHC". In: *Physics Letters B* 728 (2014), pp. 308–313. ISSN: 0370-2693. DOI: https://doi.org/10.1016/j.physletb.2013.12.011. URL: http://www.sciencedirect.com/science/article/pii/S0370269313009866.

[109] C. Lester and B. Nachman. “Bisection-based asymmetric M_{T2} computation: a higher precision calculator than existing symmetric methods”. In: *Journal of High Energy Physics* 2015.3 (Mar. 2015). ISSN: 1029-8479. DOI: 10.1007/jhep03(2015)100. URL: http://dx.doi.org/10.1007/JHEP03(2015)100.

[110] L. Cadamuro. “Search for Higgs boson pair production in the $b\bar{b}\tau^+\tau^-$ decay channel with the CMS detector at the LHC”. PhD thesis. Sept. 2017.

[111] S. Kullback and R. A. Leibler. “On Information and Sufficiency”. In: *Ann. Math. Statist.* 22.1 (Mar. 1951), pp. 79–86. DOI: 10.1214/aoms/1177729694. URL: https://doi.org/10.1214/aoms/1177729694.

[112] A. Carvalho et al. “Higgs pair production: choosing benchmarks with cluster analysis”. In: *Journal of High Energy Physics* 2016.4 (Apr. 2016), pp. 1–28. ISSN: 1029-8479. DOI: 10.1007/jhep04(2016)126. URL: http://dx.doi.org/10.1007/JHEP04(2016)126.

[113] CMS Collaboration. “Searches for a heavy scalar boson H decaying to a pair of 125 GeV Higgs bosons hh or for a heavy pseudoscalar boson A decaying to Zh, in the final states with $h \to \tau\tau$”. In: *Physics Letters B* 755 (2016), pp. 217–244. ISSN: 0370-2693. DOI: https://doi.org/10.1016/j.physletb.2016.01.056. URL: http://www.sciencedirect.com/science/article/pii/S0370269316000757.

[114] G. Strong and M. Gallinaro. “A DNN-based classification approach for enhancing the search for Higgs boson pair production in the $b\bar{b}\tau\tau$ final state in pp collision at $\sqrt{s} = 13$TeV”. In: *CMS AN -2019/188* (Aug. 2019). URL: http://cms.cern.ch/iCMS/jsp/openfile.jsp?tp=draft&files=AN2019_188_v2.pdf.

[115] D. Galbraith. “Standard Model of the Standard Model”. URL: http://davidgalbraith.org/portfolio/ux-standard-model-of-the-standard-model/.

[116] ATLAS Collaboration. “Combination of searches for Higgs boson pairs in pp collisions at $\sqrt{s}$=13 TeV with the ATLAS detector”. In: *Physics Letters B* 800 (Jan. 2020), p. 135103. ISSN: 0370-2693. DOI: 10.1016/j.physletb.2019.135103. URL: http://dx.doi.org/10.1016/j.physletb.2019.135103.

[117] E. Mobs. “The CERN accelerator complex - 2019. Complexe des accélérateurs du CERN - 2019”. In: *CERN-GRAPHICS-2019-002* (July 2019). General Photo. URL: https://cds.cern.ch/record/2684277.

[118] CMS Collaboration. “Public luminosity results”. URL: https://twiki.cern.ch/twiki/bin/view/CMSPublic/LumiPublicResults.

[119] CMS Collaboration. “Cutaway diagrams of CMS detector”. In: *CMS-OUTREACH-2019-001* (May 2019). URL: http://cds.cern.ch/record/2665537.